Proceedings of the
International Conference on Mechanical Engineering 2011
(ICME2011) 18- 20 December 2011, Dhaka, Bangladesh

ICME11-FL-054

UNSTEADY FLUID FLOW THROUGH A ROTATING CURVED SQUARE DUCT: THE CASE OF POSITIVE AND NEGATIVE ROTATION

Rabindra Nath Mondal[1], **Anup Kumar Datta**[2] **and Samir Chandra Roy**[1]

[1]Mathematics Discipline; Science, Engineering and Technology School, Khulna University, Bangladesh
[2]Department of Basic Sciences and Humanities, University of Asia Pacific, Dhanmondi, Dhaka

ABSTRACT

In this paper, a comprehensive numerical study is presented for the fully developed two-dimensional flow of viscous incompressible fluid through a rotating curved square duct with small curvature. Numerical calculations are carried out by using a spectral method and covering a wide range of the Taylor number $-1000 \le Tr \le 1000$ for two cases of the duct rotation, *Case I*: Positive rotation and *Case II*: Negative rotation. For positive rotation, we investigate the unsteady flow characteristics for the Dean number $Dn = 1000$ and $Dn = 2000$ over the Taylor number $0 \le Tr \le 1000$, and it is found that the unsteady flow undergoes in the scenario '*steady-state* $\rightarrow$ *periodic* $\rightarrow$ *multi-periodic* $\rightarrow$ *chaotic*', if *Tr* is increased in the positive direction. For negative rotation, however, we investigate the unsteady flow behavior for the Dean number $Dn = 1000$ over the Taylor number $-1000 \le Tr \le -100$, and it is found that the unsteady flow undergoes through various flow instabilities, if *Tr* is increased in the negative direction. Contours of secondary flow patterns and axial flow distribution are also obtained at several values of *Tr*, and it is found that there exist two- and four-vortex solutions if the duct is rotated in both directions.

Keywords: Curved Square Duct, Secondary Flow, Unsteady Solutions, Dean Number, Taylor Number.

1. INTRODUCTION

The study of flows and heat transfer through a curved duct is of fundamental interest because of its importance in chemical, mechanical and biological engineering. Due to engineering applications and their intricacy, the flow in a rotating curved duct has become one of the most challenging research fields of fluid mechanics. Since rotating machines were introduced into engineering applications, such as rotating systems, gas turbines, electric generators, heat exchangers, cooling system and some separation processes, scientists have paid considerable attention to study rotating curved channel flows. The readers are referred to Berger et al. [1] and Nandakumar and Masliyah [2] for some outstanding reviews on curved duct flows.

One of the interesting phenomena of the flow through a curved duct is the bifurcation of the flow because generally there exist many steady solutions due to duct curvature. Many researches have performed experimental and numerical investigations on developing and fully developed curved duct flows. An early complete bifurcation study of two-dimensional (2D) flow through a curved channel was conducted by Winters [3]. However, an extensive treatment on the flow characteristics for both the isothermal and non-isothermal flows through curved duct with rectangular cross section was performed by Mondal [4].

The flow through a rotating curved duct is another subject, which has attracted considerable attention because of its importance in engineering devices. The fluid flowing in a rotating curved duct is subjected to two forces: the Coriolis force due to rotation and the centrifugal force due to curvature. For isothermal flows of a constant property fluid, the Coriolis force tends to produce vortices while centrifugal force is purely hydrostatic. When a temperature induced variation of fluid density occurs for non-isothermal flows, both Coriolis and centrifugal type buoyancy forces can contribute to the generation of vortices (Wang and Cheng [5]). These two effects of rotation either enhance or counteract each other in a non-linear manner depending on the direction of wall heat flux and the flow domain. Therefore, the effect of system rotation is more subtle and complicated and yields new; richer features of flow

and heat transfer in general, bifurcation and stability in particular, for non-isothermal flows [6]. Recently, Mondal et al. [7] performed numerical prediction of non-isothermal flows through a rotating curved square channel with the Taylor number $0 \le Tr \le 2000$ for the Grashof number $Gr = 500$.

In the present paper, a comprehensive numerical study is presented for the flows through a rotating curved duct with square cross section. Flow characteristics are studied over a wide of the Taylor number for the Dean numbers, Dn =1000 and Dn=2000. Studying the effects of rotation on the flow characteristics is an important objective of the present study.

2. BASIC EQUATIONS

Consider a hydro-dynamically fully developed two-dimensional flow of viscous incompressible fluid through a rotating curved duct with square cross section, whose height and wide are $2h$ and $2l$, respectively. In the present case, we consider $h = l$ (square duct). The coordinate system with the relevant notation is shown in Fig. 1, where x' and y' axes are taken to be in the horizontal and vertical directions respectively, and z' is the axial direction. The system rotates at a constant angular velocity Ω_T around the y' axis. u, v and w be the velocity components in the x', y' and z' directions respectively. All the variables are non-dimensionalzed.

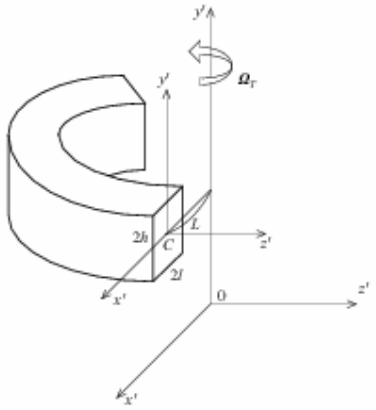

Fig 1. Coordinate system of the rotating curved square duct

The sectional stream function ψ is introduced as

$$u = \frac{1}{1+\delta x}\frac{\partial \psi}{\partial y}, \quad v = -\frac{1}{1+\delta x}\frac{\partial \psi}{\partial x} \qquad (1)$$

Then, the basic equations for the axial velocity w and the stream function ψ are expressed in terms of non-dimensional variables as:
:

$$(1+\delta x)\frac{\partial w}{\partial t} + \frac{\partial(w,\psi)}{\partial(x,y)} - Dn + \frac{\delta^2 w}{1+\delta x} = (1+\delta x)\Delta_2 w - \frac{\partial}{1+\delta x}\frac{\partial \psi}{\partial y} w + \delta \frac{\partial w}{\partial x} - \delta Tr \frac{\partial \psi}{\partial y} \qquad (2)$$

$$\left(\Delta_2 - \frac{\delta}{1+\delta x}\frac{\partial}{\partial x}\right)\frac{\partial \psi}{\partial t} = -\frac{1}{(1+\delta x)}\frac{\partial(\Delta_2\psi,\psi)}{\partial(x,y)} + \frac{\delta}{(1+\delta x)^2}\left[\frac{\partial \psi}{\partial y}\left(2\Delta_2\psi - \frac{3\delta}{1+\delta x}\frac{\partial \psi}{\partial x} + \frac{\partial^2 \psi}{\partial x^2}\right) - \frac{\partial \psi}{\partial x}\frac{\partial^2 \psi}{\partial x \partial y}\right] + \frac{\delta}{(1+\delta x)^2}\left[3\delta\frac{\partial^2 \psi}{\partial x^2} - \frac{3\delta^2}{1+\delta x}\frac{\partial \psi}{\partial x}\right] - \frac{2\delta}{1+\delta x}\frac{\partial}{\partial x}\Delta_2\psi + w\frac{\partial w}{\partial y} + \Delta_2{}^2\psi + \frac{1}{2}Tr\frac{\partial w}{\partial y}, \qquad (3)$$

where

$$\Delta_2 \equiv \frac{\partial^2}{\partial x^2} + \frac{\partial^2}{\partial y^2},$$

$$\frac{\partial(T,\psi)}{\partial(x,y)} \equiv \frac{\partial f}{\partial x}\frac{\partial g}{\partial y} - \frac{\partial f}{\partial y}\frac{\partial g}{\partial x}$$

The non-dimensional parameters Dn, the Dean number and Tr, the Taylor number, which appear in equation (2) and (3) are defined as:

$$Dn = \frac{Gl^3}{\mu\upsilon}\sqrt{\frac{2l}{L}}, \quad Tr = \frac{2\sqrt{2\delta}\,\Omega_T l^3}{\upsilon\delta} \qquad (4)$$

where the parameters denote their usual meaning.

The rigid boundary conditions for w and ψ are used as

$$w(\pm 1, y) = w(x, \pm 1) = \psi(\pm 1, y) = \psi(x, \pm 1) = \frac{\partial \psi}{\partial x}(\pm 1, y) = \frac{\partial \psi}{\partial y}(x, \pm 1) = 0 \qquad (5)$$

There is a class of solutions which satisfy the following symmetry condition with respect to the horizontal plane $y = 0$.

$$\left.\begin{aligned} &(x, y, t) \Rightarrow w(x, -y, t), \\ &\psi(x, y, t) \Rightarrow -\psi(x, -y, t) \end{aligned}\right\} \qquad (6)$$

The solution which satisfies condition (7) is called a symmetric solution and that does not an asymmetric solution. Note that, Equations (2) - (3) are invariant under the transformation of the variables

$$\left.\begin{aligned} &y \Rightarrow -y \\ &w(x, y, t) \Rightarrow w(x, -y, t), \\ &\psi(x, y, t) \Rightarrow -\psi(x, -y, t \end{aligned}\right\} \qquad (7)$$

Equations (2) and (3) would serve as the basic governing equations which will be solved numerically.

3. NUMERICAL METHODS

In order to solve the Equations (2) and (3) numerically, the spectral method is used. By this method the expansion functions $\phi_n(x)$ and $\psi_n(x)$ are expressed as

$$\left.\begin{aligned}\phi_n(x) &= (1-x^2)C_n(x),\\ \psi_n(x) &= (1-x^2)^2 C_n(x)\end{aligned}\right\} \tag{8}$$

Where $C_n(x) = \cos(n\cos^{-1}(x))$ is the n^{th} order Chebyshev polynomial. $w(x,y,t)$, $\psi(x,y,t)$ are expanded in terms of the expansion functions $\phi_n(x)$ and $\psi_n(x)$ as

$$\left.\begin{aligned}w(x,y,t) &= \sum_{m=0}^{M}\sum_{n=0}^{N} w_{mn}(t)\varphi_m(x)\varphi_n(y)\\ \psi(x,y,t) &= \sum_{m=0}^{M}\sum_{n=0}^{N} \psi_{mn}(t)\psi_m(x)\psi_n(y).\end{aligned}\right\} \tag{9}$$

where M and N are the truncation numbers in the x and y directions respectively.

First, steady solutions are obtained by the Newton-Rapshon iteration method and then linear stability of the steady solutions is investigated against only two-dimensional ($z-$ independent) perturbations. Finally, in order to calculate the unsteady solutions, the Crank-Nicolson and Adams-Bashforth methods together with the function expansion (10) and the collocation methods are applied to Eqs. (2) and (3).

4. RESISTANT COEFFICIENT

The resistant coefficient λ is used as the representative quantity of the flow state and is generally used in fluids engineering, defined as

$$\frac{P_1^* - P_{21}^*}{\Delta_{z^*}} = \frac{\lambda}{d_h^*}\frac{1}{2}\rho\langle\omega^*\rangle^2 \tag{10}$$

where quantities with an P_1^* be asterisk denote dimensional ones, $\langle\ \rangle$ stands for the mean over the cross section of the duct and $d_h^* = 4(2d\times 2dl)/(4d+4dl)$ is the hydraulic diameter. The main axial velocity $\langle\omega^*\rangle$ is calculated by

$$\langle\omega^*\rangle = \frac{\nu}{4\sqrt{2\delta d}}\int_{-1}^{1}dx\int_{-1}^{1}\omega(x,y,t)dy \tag{11}$$

Since $\left(P_1^* - P_2^*\right)/\Delta_{z^*} = G$, λ is related to the mean non-dimensional axial velocity $\langle\omega\rangle$ as

$$\lambda = \frac{8l\sqrt{2\delta}Dn}{(1+l)\langle\omega\rangle^2} \tag{12}$$

where $\langle\omega\rangle = \sqrt{2\delta d}\,\langle\omega^*\rangle/\nu$.

5. RESULTS AND DISCUSSION

5.1 Case I: Positive Rotation

In order to study the non-linear behavior of the unsteady solutions, time-evolution calculations are performed for Dn=1000 over the Taylor number $0 \le Tr \le 1000$. It is found that the flow is periodic for $0 \le Tr \le 140$. Figure 2(a) shows time evolution of λ for Dn = 1000 and Tr = 0, where it is seen that the flow is time periodic, which is well justified by drawing the phase spaces as shown in Fig. 2(b). Then, in order to see the change of the flow characteristics, as time proceeds, contours of typical secondary flow patterns and axial flow distributions are shown in Fig. 3, where it is seen that the periodic solution at Dn = 1000 and Tr = 0 oscillates between asymmetric two- and four-vortex solutions. It is found that the flow is steady-state for $150 \le Tr \le 630$. Figure 4(a) shows steady-state solution at *Tr* = 150. Secondary flow patterns, as shown in Fig. 4(b), show that it is a symmetric two-vortex solution. If *Tr* is increased further, i.e. for $640 \le Tr \le 890$, the flow becomes periodic. However, the flow becomes chaotic at the large values of Tr, $900 \le Tr \le 1000$.

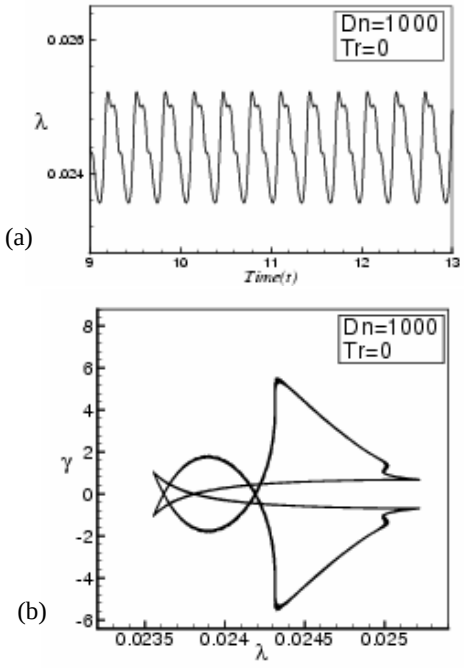

Fig 2. (a) Time evolution of λ for Dn = 1000 and Tr = 0. (b) Phase Plots in the $\lambda-\gamma$ plane for Dn = 1000 and *Tr* = 0, where $\gamma = \iint \psi\, dxdy$.

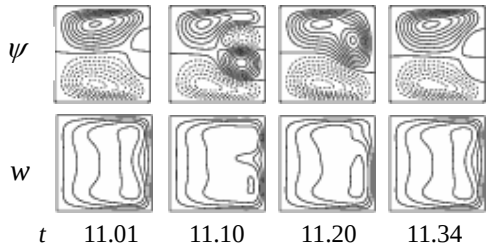

Fig 3. Contours of secondary flow patterns (top) and axial flow distribution (bottom) for Dn=1000 and *Tr* =0.

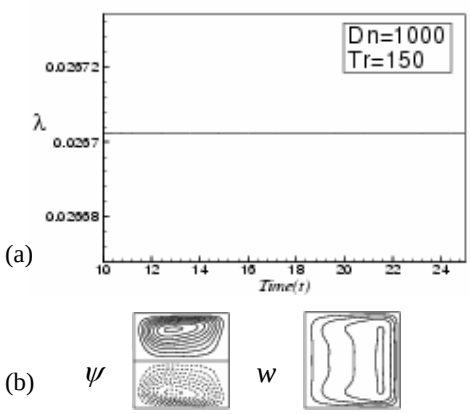

Fig 4. (a) Unsteady solutions for Dn=1000 and Tr = 150. (b) Contours of secondary flow and axial flow at *t* = 20.

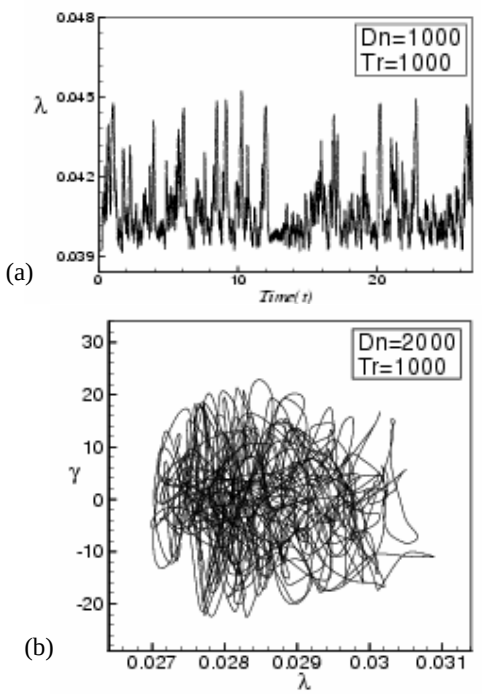

Fig 5. (a) Time evolution of λ for Dn=1000 and Tr = 1000. (b) Phase spaces in the $\lambda - \gamma$ plane.

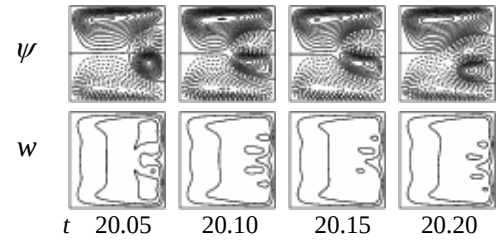

Fig 6. Contours of secondary flow patterns and axial flow distribution for Dn = 1000 and Tr = 1000.

Figure 5(a) shows time-evolution of λ for Dn = 1000 and Tr = 1000, where it is seen that flow oscillates irregularly that is the flow is chaotic. The corresponding phase space is shown in Fig. 5(b), which shows the chaotic orbit. Then contours of secondary flow patterns and axial flow distributions are shown in Fig. 6, where it is seen that the chaotic solution at Dn = 1000 and *Tr* = 1000 oscillates between four-vortex solutions.

Then we investigate unsteady solutions for Dn=2000 and $0 \le Tr \le 1000$. It is found that the flow is steady-state for $0 \le Tr \le 80$. Figure 7(a) shows time evolution of λ for Dn = 2000 and Tr = 0, where it is seen that the flow is steady-state. Since the flow is steady-state, a single contour of secondary flow pattern and axial flow distribution is shown in Fig. 7(b). As seen in Fig. 7(b), the flow is a symmetric two-vortex solution. It is found that the flow is periodic and multi-periodic for $90 \le Tr \le 530$. Figure 8(a) shows periodic oscillation at Dn = 2000, Tr =90. Contours of secondary flow patterns and axial flow distribution for Dn = 2000 and Tr = 90 are shown in Fig. 8(b), where it is seen that the periodic oscillation as a symmetric two-vortex solution. If *Tr* is increased further, i.e. $540 \le Tr \le 1000$, the flow becomes chaotic. Figure 9(a) shows unsteady solutions for Dn=2000 and Tr = 1000 and it is found that the flow is chaotic, which is justified by the phase plots as shown in Fig. 9(b).

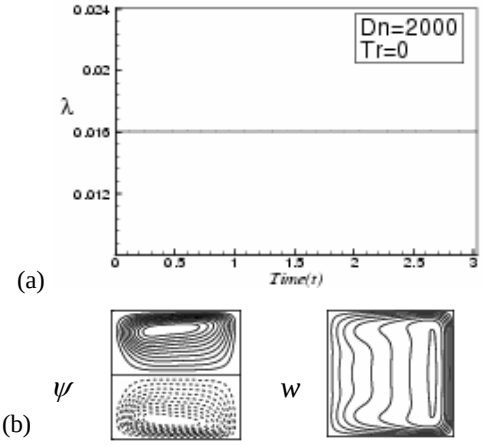

Fig 7 (a) Time evolution of λ for the unsteady solutions at Dn=2000 and Tr = 0. (b) Contours of secondary flow and axial flow distribution at *t* = 10.

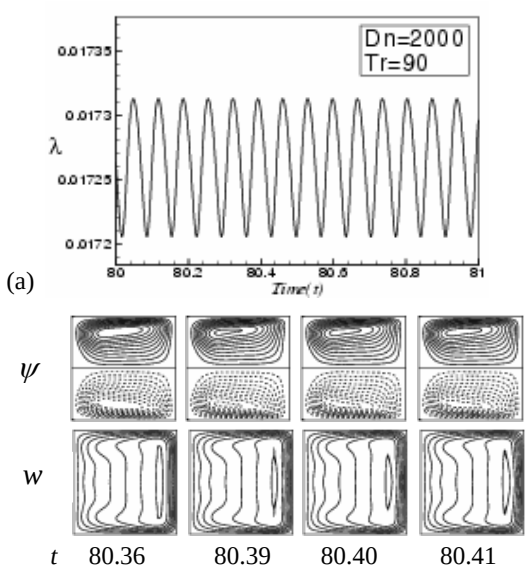

Fig 8. (a) Unsteady solutions for Dn=2000 and Tr = 90. (b) Contours of secondary flow patterns and axial flow distribution for Dn = 2000 and Tr = 90.

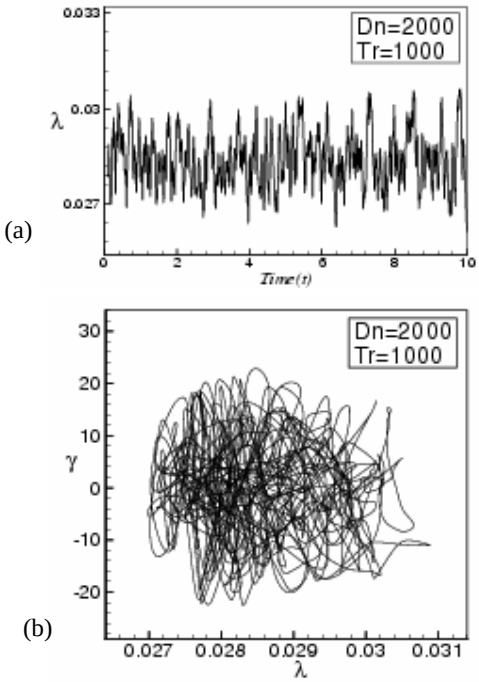

Fig 9. (a) Time evolution of λ for the unsteady solutions for Dn=2000 and Tr = 1000. (b) Phase spaces for Dn = 2000 and Tr = 1000.

5.2 Case II: Negative Rotation

We rotate the duct in the negative direction for $-100 \le Tr \le -1000$ and investigate the unsteady flow behavior for Dn = 1000. Time evolutions of λ for $-100 \le Tr \le -150$ show that the flow is periodic or multi-periodic. Figure 10(a) shows that the flow is periodic for Dn = 1000 and *Tr* = -100, but its phase space shows (Fig. 10(b)) that it is multi-periodic. Then, in order to see the change of the flow characteristics, as time proceeds, contours of typical secondary flow patterns and axial flow distributions for Tr = -100 are shown in Fig. 11, where it is seen that the periodic solution at Dn = 1000 and Tr = -100 oscillates between three- and four-vortex solutions. It is found that the flow oscillates multi-periodically at Dn = 1000 and Tr = -150 as shown in Fig. 12(a). It is well justified by the phase plots as shown in Fig. 12(b), where multi-periodic orbit is seen. The associate secondary flow patterns and axial flow distributions are shown in 13, where it is seen that the multi-period oscillation at Tr = -150 is the asymmetric four-vortex solutions. Next, the time evolution of λ is performed for $-155 \le Tr \le -380$ and it is found that the unsteady flow is a steady-state solution. If *Tr* is increased more in the negative direction ($-390 \le Tr \le -540$), the flow becomes periodic first and then multi-periodic. However, if Tr is increased further in the negative direction, the flow turns into steady-state solution. Figure 14(a) shows time evolution of λ for Tr = -540 at Dn = 1000. It is seen that the unsteady flow at Tr = -540 is a multi-periodic solution, which is well justified by the phase spaces as shown in Fig. 14(b). Then, contours of typical secondary flow patterns and axial flow distributions for Tr = -540 are shown in Fig. 15, where it is seen that the multi-periodic solution at Dn = 1000 and Tr = -540 oscillates between two- and four-vortex solutions. Axial flow is consistent with the secondary vortices. We studied time evolution of λ for $-550 \le Tr \le -950$ and it is found that the flow is a steady state solution in this range. If *Tr* is increased further in the negative direction, the steady-state oscillation turns into a periodic oscillation. It is found that the transition from steady-state to periodic oscillation occurs between Tr = -950 and Tr = -960.

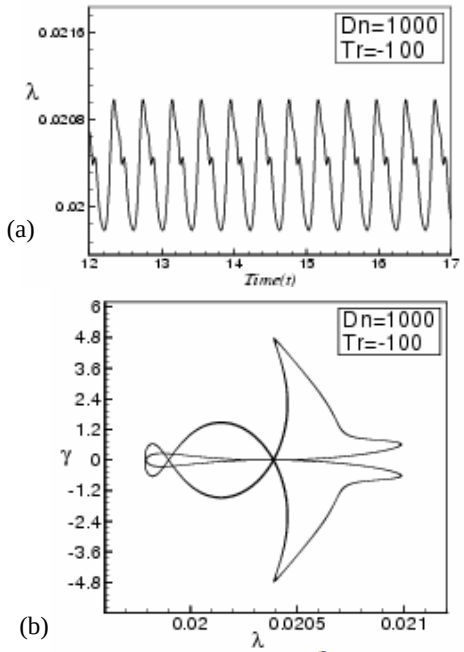

Fig 10. (a) Time evolution of λ for the unsteady solutions for Dn=1000 and Tr = -100. (b) Phase Plots in the $\lambda - \gamma$ plane for Dn = 1000 and Tr = -100.

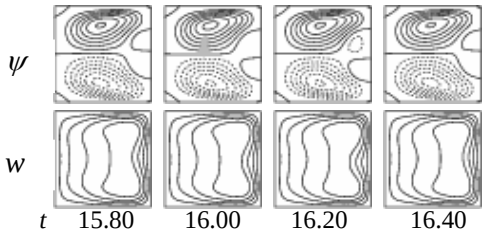

Fig 11. Contours of secondary flow patterns (top) and axial flow distribution (bottom) for Dn = 1000 and Tr = -100.

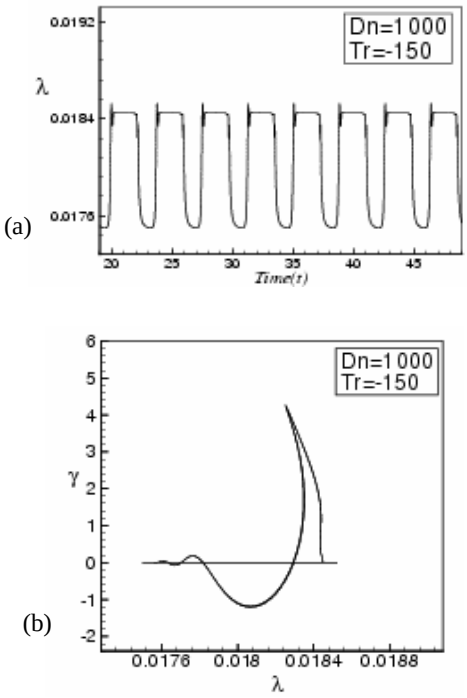

Fig 12. (a) Unsteady solutions for Dn=1000 and Tr = -150. (b) Phase spaces in for Dn = 1000 and Tr = -150.

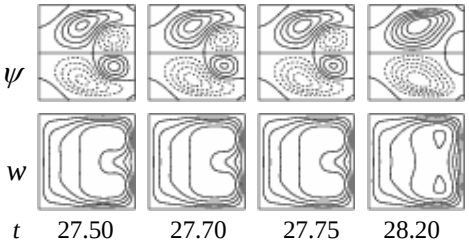

Fig 13. Contours of secondary flow (top) and axial flow distribution (bottom) for Dn=1000 and Tr =-150.

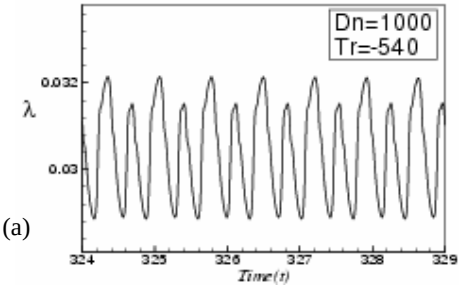

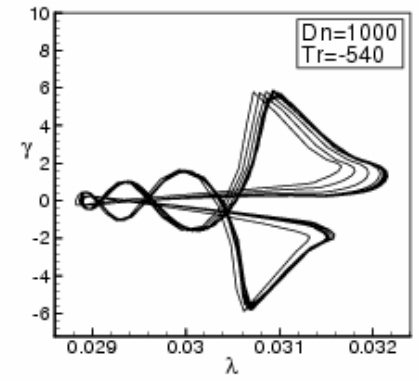

Fig 14. (a) Unsteady solutions for Dn=1000 and Tr = -540. (b) Phase spaces for Dn = 1000 and Tr = -540.

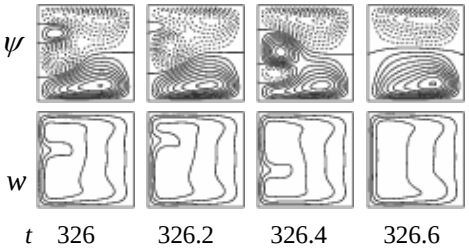

Fig 15 Contours of secondary flow (top) and axial flow distribution (bottom) for Dn = 1000 and Tr = -540.

6. CONCLUSIONS

In this study, a numerical simulation is presented for the fully developed two-dimensional flow of viscous incompressible fluid through a rotating curved square duct for the Dean numbers, Dn = 1000 and Dn = 2000 for both the positive and negative rotation of the duct. Spectral method is used as a basic tool to solve the system of non-linear differential equations. We studied the unsteady solutions for Dn = 1000 and Dn = 2000 for positive rotation at $0 \le Tr \le 1000$. It is found that, for Dn = 1000 the unsteady flow undergoes in the scenario '*multi-periodic* $\rightarrow$ *steady-state* $\rightarrow$ *periodic* $\rightarrow$ *multi-periodic* $\rightarrow$ *chaotic*' if Tr is increased in the positive direction. For Dn = 2000, however, the steady flow turns into chaotic flow through periodic and multi-periodic oscillation. The secondary flow is two-, three- and four-vortex solutions. For the negative rotation ($-1000 \le Tr \le -100$) at Dn = 1000, it is found that the unsteady flow undergoes '*multi-periodic* $\rightarrow$ *steady-state* $\rightarrow$ *periodic* $\rightarrow$ *multi-periodic* $\rightarrow$ *chaotic*' if Tr is increased in the negative direction, and the flow oscillated between two- , four- and six-vortex solution. Drawing the phase spaces was found to be very fruitful to investigate the unsteady flow characteristics.

7. REFERENCES

1. Berger, S.A., Talbot, L., Yao, L. S. (1983). Flow in Curved Pipes, *Annu. Rev. Fluid. Mech.*, Vol. 35, pp. 461-512.
2. Nandakumar, K. and Masliyah, J. H. (1986). Swirling Flow and Heat Transfer in Coiled and

Twisted Pipes, *Adv. Transport Process.*, Vol. 4, pp.49-112.
3. Winters, K. H. (1987). Bifurcation Study of Laminar Flow in a Curved Tube of Rectangular Cross-section, *Journal of Fluid Mech.*, Vol. 180, pp.343-369.
4. Mondal, R. N. (2006) Isothermal and Non-isothermal Flows through Curved ducts with Square and Rectangular Cross Sections, *Ph.D. Thesis*, Department of Mechanical Engineering, Okayama University, Japan.
5. Wang, L. Q. and Cheng, K.C. (1996). Flow Transitions and Combined Free and Forced Convective Heat Transfer in Rotating Curved Channels: the Case of Positive Rotation, *Phys. of Fluids*, Vol. 8, pp.1553-1573.
6. Mondal, R. N., Alam M. M. and Yanase, S. (2007). Numerical prediction of non-isothermal flows through a rotating curved duct with square cross section, *Thommasat Int. J. Sci and Tech.*, Vol. 12, No. 3, pp. 24-43.
7. Mondal, R. N., Datta, A. K and Mondal, B. (2011). Bifurcation study of thermal Flows through a rotating curved square duct, *Bangladesh Journal of Scientific and Industrial Research*, (accepted).

8. MAILING ADRESS

Rabindra Nath Mondal
Mathematics Discipline; Science, Engineering and Technology School,
Khulna University,
Khulna-9208, Bangladesh
Cell Phone: 0088-01710851580,
Fax: 0088-041-731244
Email: rnmondal71@yahoo.com